12

The gradient descent method in the problem of charge distribution over the surfaces of three concentric tori

© V.Yu. Sakharov, A.A. Tikhonov ¶

St. Petersburg State University, St. Petersburg, Russia
¶ e-mail: a.tikhonov@spbu.ru

Received July 31, 2024
Revised December 20, 2024
Accepted December 23, 2024

A system of three circular concentric non-touching tori is considered. An electrostatic charge can be applied to each of the tori. The problem is to find the density of charge distribution over the surfaces of the tori, taking into account the Coulomb interaction between the surfaces. The required density is found by the method of successive approximations based on the fact that in the static case, at each of the points on the surface of each of the tori, the total tangential strength of the Coulomb forces is zero. The corresponding functional is constructed, the problem of numerical minimization of which is solved by the gradient descent method.

Keywords: torus, electrostatic charge, surface density, gradient descent method.

DOI: 10.61011/TP.2025.06.61384.247-24

Introduction

Due to the intensive study and exploration of outer cosmic space, including in conditions of longer lasting manned flights, the problem of ensuring the radiation safety of space flights is becoming more urgent. There is an obvious need to improve the existing and develop fundamentally new approaches to ensuring radiation protection of habitable compartments and onboard spacecraft equipment against harmful effects of galactic cosmic rays, radiation from the Earth's radiation belts, chromospheric solar bursts, etc. One such approach is to create active protection systems that use the ability of electric and magnetic fields to change the direction of the moving charged particles and deflect them from the surface of a spacecraft [1–4].

As theoretical and experimental studies show, these systems are set apart from the passive radiation protection systems traditionally used in practice based on the use of absorbing properties of materials. Active protection provides a significantly lower level of generated secondary radiation and a way higher order of radiation attenuation per unit mass. Therefore, it not only allows to significantly reduce the total weight of a spacecraft, but also proves to be extremely effective for protection of large volumes.

One of the most promising ways to provide active radiation protection is to implement an electrostatic discharge (ESD) system based on the use of an electrostatically charged shield covering the protected volume, which has a certain potential relative to its environment and deflects the incident flows of charged particles away from its surface [5,6]. For the implementation of protective shields, it was proposed to use a thin metallized film stretched over a lightweight and durable spherical or cylindrical frame [5]. Also an idea of the module structure of ESD shield was suggested allowing to cover the surface of a spacecraft having complex shape [6]. In general, both the theoretical studies and the results of experiments carried out in space on bio-satellites „Kosmos" (from 605 to 2229) and spacecrafts „Prognoz" [6–8], have proved that effective ESD control is technically feasible with the present day's state of the art. It has been established that the power consumed by the ESD is low compared to the total reserve of energy resources of the spacecraft. It should be also emphasized that experiments made on the bio-satellite „Kosmos"-936 have proved that ESD could operate in a self-charge mode [9]. This finding indicates high dependability of the ESD systems.

Foreign studies concerning the development of active anti-radiation protection systems also pay attention to ESD systems (see, for example, the review [10] and the literature cited in it). At that it is mentioned that technical feasibility of ESD may be somewhat troublesome. For example, these difficulties may be associated with maintaining the required high electrostatic potentials in conditions of a continuous flow of conductive plasma particles in the near-Earth space. In some foreign papers, ESD was even rejected as inoperable. This, as noted in [11], was based on the false assumption that radial symmetry of the electrostatic field is necessary to ensure the isotropic protection of a spacecraft. it was demonstrated that ESD protection is feasible when compiled of several shields. It is noted that the combination of electric monopoles, dipoles, quadrupoles and more complex structures makes it possible to generate an electrostatic field that effectively protects the spacecraft from ionizing radiation. For instance, in paper [11] an ESD system is described having 18 electrostatically charged spheres. At

the same time, proper use of physical asymmetry makes it possible to repel both electrons and positively charged ions without creating excessive secondary radiation. The rapid deployment of such fields does not require heavy structures with passive shields or concentric shells of charges, and the vacuum breakdown limit can be easily overcome [11].

The continued research aimed at clarifying the feasibility of ESD in terms of energy supply on board the spacecraft, as well as the search for suitable materials for electrostatic screens according to UV radiation resistance criteria, resistance to impact of microparticles of space debris, the ability to resist tensile loads, electrical strength all this resulted in finding the acceptable solutions and development of new ESD options [12], but at the same time it revealed some new problems.

The first of them is that even with the use of the most modern and advanced materials for the construction of ESD with 12- charged spheres, the total mass of the ESD system turns out to be too large for practical use of the system compared to a system based on passive protection where absorbing screens are used [12].

The second problem is that most of the works for creation and testing of ESD systems in space successfully carried out in the USSR [1–3,5–9], was dealing with protection against radiation with the energy level from 10 to 100 MeV. Now we understand that the real problem is radiation with energy from 1 to 2 GeV. So, the issue is scaling, both in terms of energy and in terms of the size of the ESD. Is it possible to create an ESD capable of operating at such high levels of energy consumption, and can it protect the entire spacecraft?

In the process of studying this issue, a new conceptual design was proposed, which should be evaluated in the course of upcoming studies, taking into account the complexity and mass of the system. It is based on a torus surrounding the spacecraft [12]. An ESP configuration is proposed, which consists of a torus charged to a high negative voltage surrounding the spacecraft and a set of positively charged spheres. Van de Graaff generators have been proposed as a mechanism for moving charge from a spacecraft to a torus to create fields necessary to protect the spacecraft.

Continued research on electrostatic shielding led to the development of the idea of using toroidal surfaces by switching to a configuration based on the use of several toroidal surfaces (or toroidal rings, as they are titled in [13]). Analytical and numerical studies show that with the help of such electrostatic configurations, the radiation from solar bursts can be practically eliminated. It is also shown that the probability of ionizing particles penetrating into toroidal surfaces is significantly reduced compared to simpler spherical structures. It is established that the sizes and the ratio of the radii of the toroidal surfaces can vary and may be optimized to achieve higher radiation protection [13].

During preliminary analysis of the effectiveness of the electrostatic protection system, it is usually limited to finding the electric potential in the vicinity of the charged surface. When the system has charged surfaces, where the charges may have a mutual effect on the overall charge distribution, this task is very difficult. In this view, the classical solution method based on solving the Dirichlet problem for the Laplace equation may be practically inapplicable, and therefore other approaches are used. Thus, for example, in paper [14], when analyzing the effectiveness of an ESD containing the above-mentioned system of spherical surfaces, the problem of finding the electric potential is solved using the method of purely imaginary charges.

When considering an ESD with a system of toroidal surfaces, we note that for a single charged torus, the potential in the outer region, found analytically by solving the Dirichlet problem for the Laplace equation, is given, for example, in papers [13,15]. In [13], this solution is used to find the charge that needs to be distributed on the surface of the torus in order to maintain a constant set potential value on this surface. For a promising ESD system containing three concentric toroidal surfaces [13], the task of finding the potential becomes much more complicated because of mutual influence of charges distributed over the surfaces of the tori. Therefore, when analyzing the effectiveness of such an ESD, a numerical approach based on the finite element method is used.

The purpose of this study is to analyze the dynamics of a spacecraft equipped with an ESD system that includes three concentric toroidal surfaces. At the same time, to analyze the electrodynamic effects resulting from the interaction of charged surfaces with the Earth's magnetic field, it is not enough to know the electric potential of a system of charged toroidal surfaces. We need to know the density of charge distributions over the surfaces of the tori.

For a single torus, the problem of finding the charge distribution density over the surface can be solved after finding the derivative on the surface of the torus from the potential in the outer part of the torus [16]. The expression for the potential, as noted above, is outlined in [13,15], where it is given as a Fourier series expansion, the terms of which are expressed in terms of Legendre functions of half-integer orders of the first and second kinds.

In this paper, we consider a system of three concentric non-intersecting hollow electrically conductive tori. An electrostatic charge may be supplied to each of these tori. The task is to find the densities of charge distributions over the surfaces of these tori. To solve the problem, it is proposed to directly find the densities of charge distributions (bypassing the electric potential) using the method of successive approximations, based on the fact that

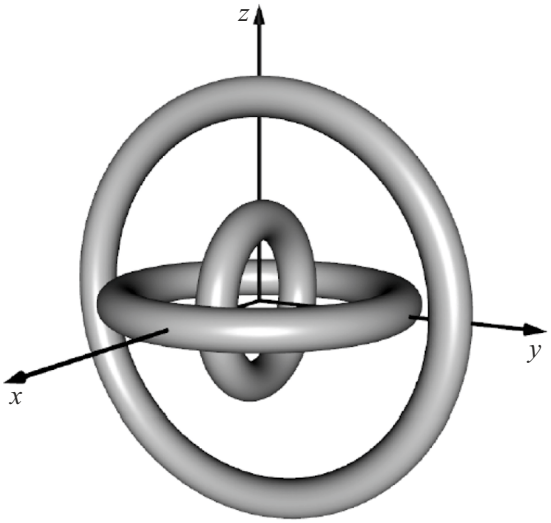

Figure 1. Three mutually perpendicular non-intersecting tori.

in the static case, at each of the points on the surface of each of the tori, the total tangential tension of the Coulomb forces is zero. At the same time, the interaction of charge distributions on different tori is taken into account in this study.

1. Mathematical model

A system of three non-intersecting hollow toroidal shells made of a conductive material, having a common center and oriented parallel to mutually perpendicular planes is considered (Fig. 1).

Let's denote by index i the elements of the torus on which the charge distribution is adjusted, and by index j the elements of the torus on which the tangential component of tension is minimized. To avoid confusion, these indexes will take alphabetic values instead of numeric ones $i, j = S, M, L$ for Small, Medium, and Large volumes, respectively.

An orthogonal coordinate system (φ, ψ) is introduced on each of the three toroidal surfaces (Fig. 2). Cartesian coordinates of a point on a toroidal surface are easily expressed using a cylindrical coordinate $\rho = R + r \cdot \cos\psi$:

$$\begin{cases} x = \rho \cdot \cos\varphi = (R + r \cdot \cos\psi) \cdot \cos\varphi, \\ y = \rho \cdot \sin\varphi = (R + r \cdot \cos\psi) \cdot \sin\varphi, \\ z = r \cdot \sin\psi. \end{cases} \tag{1}$$

If, for certainty, we assume that the medium torus is oriented parallel to the coordinate plane Oxy (Fig. 2 corresponds exactly to this case), then such a coordinate system will look as

$$\begin{cases} x_M = (R_M + r_M \cdot \cos\psi_M) \cdot \cos\varphi_M, \\ y_M = (R_M + r_M \cdot \cos\psi_M) \cdot \sin\varphi_M, \\ z_M = r_M \cdot \sin\psi_M. \end{cases} \tag{2}$$

Here r_M is the radius of the generating circle, and R_M is the distance from the center of the generating circle to the axis of symmetry perpendicular to the orientation plane, $\varphi \in [0, 2\pi]$, $\psi \in [0, 2\pi]$. For the small torus, which we assume to be oriented parallel to the coordinate plane Oxz, the coordinate system will be

$$\begin{cases} x_S = (R_S + r_S \cdot \cos\psi_S) \cdot \cos\varphi_S, \\ y_S = r_S \cdot \sin\psi_S, \\ z_S = (R_S + r_S \cdot \cos\psi_S) \cdot \sin\varphi_S. \end{cases} \tag{3}$$

And for a large torus oriented parallel to the coordinate plane Oyz, the expression will be

$$\begin{cases} x_L = r_L \cdot \sin\psi_L, \\ y_L = (R_L + r_L \cdot \cos\psi_L) \cdot \sin\varphi_L, \\ z_L = (R_L + r_L \cdot \cos\psi_L) \cdot \cos\varphi_L. \end{cases} \tag{4}$$

For each point $M_j(\tilde{x}_j, \tilde{y}_j, \tilde{z}_j)$ of each of the three toroidal surfaces, the total tangential strength of the electrostatic field generated by charges distributed over the surfaces of all three tori shall be equal to zero vector. Here and further, the tilde sign will refer to the coordinates of those points at which the electrostatic field strength is calculated. If we denote $q_i(\varphi_i, \psi_i)$ the density of the charge distribution at the point $N_i(x_i, y_i, z_i)$, and $\overrightarrow{\tau_{ij}}(\varphi_i, \psi_i, \tilde{\varphi}_j, \tilde{\psi}_j)$ — the projection of the vector $\overrightarrow{N_i M_j}$ on the tangent plane to the j-th toroidal surface containing the point M_j, then this tension can be represented as the sum of integrals over the surfaces of three tori (k is Coulomb's constant, which in this problem can be shortened):

$$\overrightarrow{E_{\tau j}} = k \sum_{i=S,M,L} r_i \int_0^{2\pi} (R_i + r_i \cdot \cos\psi_i)\, d\psi_i \int_0^{2\pi} \frac{q_i \cdot \overrightarrow{\tau_{ij}}}{|N_i M_j|^3} d\varphi_i = \overrightarrow{0}. \tag{5}$$

Vector $\overrightarrow{N_i M_j}$ will have nine various expressions:

$$\overrightarrow{N_S M_S} = \begin{pmatrix} (R_S + r_S \cdot \cos\tilde{\psi}_S) \cdot \cos\tilde{\varphi}_S - (R_S + r_S \cdot \cos\psi_S) \cdot \cos\varphi_S \\ r_S \cdot \sin\tilde{\psi}_S - r_S \cdot \sin\psi_S \\ (R_S + r_S \cdot \cos\tilde{\psi}_S) \cdot \sin - \tilde{\varphi}_S\, (R_S + r_S \cdot \cos\psi_S) \cdot \sin\varphi_S \end{pmatrix}, \tag{6}$$

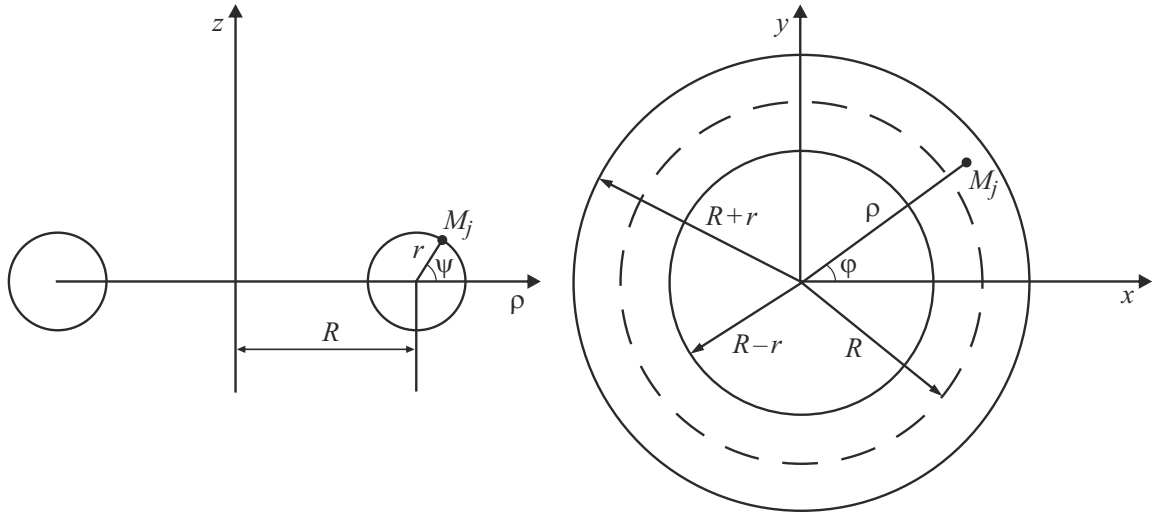

Figure 2. The coordinate system on a toroidal shell.

$$\overrightarrow{N_M M_S} = \begin{pmatrix} \left(R_S + r_S \cdot \cos\tilde{\psi}_S\right) \cdot \cos\tilde{\varphi}_S - \left(R_M + r_M \cdot \cos\psi_M\right) \cdot \cos\varphi_M \\ r_S \cdot \sin\tilde{\psi}_S - \left(R_M + r_M \cdot \cos\psi_M\right) \cdot \sin\varphi_M \\ \left(R_S + r_S \cdot \cos\tilde{\psi}_S\right) \cdot \sin\tilde{\varphi}_S - r_M \cdot \sin\psi_M \end{pmatrix}, \tag{7}$$

$$\overrightarrow{N_L M_S} = \begin{pmatrix} \left(R_S + r_S \cdot \cos\tilde{\psi}_S\right) \cdot \cos\tilde{\varphi}_S - r_L \cdot \sin\psi_L \\ r_S \cdot \sin\tilde{\psi}_S - \left(R_L + r_L \cdot \cos\psi_L\right) \cdot \sin\varphi_L \\ \left(R_S + r_S \cdot \cos\tilde{\psi}_S\right) \cdot \sin\tilde{\varphi}_S - \left(R_L + r_L \cdot \cos\psi_L\right) \cdot \cos\varphi_L \end{pmatrix}, \tag{8}$$

$$\overrightarrow{N_S M_M} = \begin{pmatrix} \left(R_M + r_M \cdot \cos\tilde{\psi}_M\right) \cdot \cos\tilde{\varphi}_M - \left(R_S + r_S \cdot \cos\psi_S\right) \cdot \cos\varphi_S \\ \left(R_M + r_M \cdot \cos\tilde{\psi}_M\right) \cdot \sin\tilde{\varphi}_M - r_S \cdot \sin\psi_S \\ r_M \cdot \sin\tilde{\psi}_M - \left(R_S + r_S \cdot \cos\psi_S\right) \cdot \sin\varphi_S \end{pmatrix}, \tag{9}$$

$$\overrightarrow{N_M M_M} = \begin{pmatrix} \left(R_M + r_M \cdot \cos\tilde{\psi}_M\right) \cdot \cos\tilde{\varphi}_M - \left(R_M + r_M \cdot \cos\psi_M\right) \cdot \cos\varphi_M \\ \left(R_M + r_M \cdot \cos\tilde{\psi}_M\right) \cdot \sin\tilde{\varphi}_M - \left(R_M + r_M \cdot \cos\psi_M\right) \cdot \sin\varphi_M \\ r_M \cdot \sin\tilde{\psi}_M - r_M \cdot \sin\psi_M \end{pmatrix}, \tag{10}$$

$$\overrightarrow{N_L M_M} = \begin{pmatrix} \left(R_M + r_M \cdot \cos\tilde{\psi}_M\right) \cdot \cos\tilde{\varphi}_M - r_L \cdot \sin\psi_L \\ \left(R_M + r_M \cdot \cos\tilde{\psi}_M\right) \cdot \sin\tilde{\varphi}_M - \left(R_L + r_L \cdot \cos\psi_L\right) \cdot \sin\varphi_L \\ r_M \cdot \sin\tilde{\psi}_M - \left(R_L + r_L \cdot \cos\psi_L\right) \cdot \cos\varphi_L \end{pmatrix}, \tag{11}$$

$$\overrightarrow{N_S M_L} = \begin{pmatrix} r_L \cdot \sin\tilde{\psi}_L - \left(R_S + r_S \cdot \cos\psi_S\right) \cdot \cos\varphi_S \\ \left(R_L + r_L \cdot \cos\tilde{\psi}_L\right) \cdot \sin\tilde{\varphi}_L - r_S \cdot \sin\psi_S \\ \left(R_L + r_L \cdot \cos\tilde{\psi}_L\right) \cdot \cos\tilde{\varphi}_L - \left(R_S + r_S \cdot \cos\psi_S\right) \cdot \sin\varphi_S \end{pmatrix}, \tag{12}$$

$$\overrightarrow{N_M M_L} = \begin{pmatrix} r_L \cdot \sin\tilde{\psi}_L - \left(R_M + r_M \cdot \cos\psi_M\right) \cdot \cos\varphi_M \\ \left(R_L + r_L \cdot \cos\tilde{\psi}_L\right) \cdot \sin\tilde{\varphi}_L - \left(R_M + r_M \cdot \cos\psi_M\right) \cdot \sin\varphi_M \\ \left(R_L + r_L \cdot \cos\tilde{\psi}_L\right) \cdot \cos\tilde{\varphi}_L - r_M \cdot \sin\psi_M \end{pmatrix}, \tag{13}$$

$$\overrightarrow{N_L M_L} = \begin{pmatrix} r_L \cdot \sin\tilde{\psi}_L - r_L \cdot \sin\psi_L \\ \left(R_L + r_L \cdot \cos\tilde{\psi}_L\right) \cdot \sin\tilde{\varphi}_L - \left(R_L + r_L \cdot \cos\psi_L\right) \cdot \sin\varphi_L \\ \left(R_L + r_L \cdot \cos\tilde{\psi}_L\right) \cdot \cos\tilde{\varphi}_L - \left(R_L + r_L \cdot \cos\psi_L\right) \cdot \cos\varphi_L \end{pmatrix}. \tag{14}$$

The projection $\overrightarrow{\tau_{ij}}$ can be found from the formula

$$\overrightarrow{\tau_{ij}} = \overrightarrow{N_i M_j} - \left(\overrightarrow{N_i M_j} \cdot \overrightarrow{n_j}\right) \cdot \overrightarrow{n_j}, \tag{15}$$

where $\overrightarrow{n_j}\left(\tilde{\varphi}_j, \tilde{\psi}_j\right)$ is the normal vector to the corresponding toroidal surface in point M_j. For the medium toroidal surface $\overrightarrow{n_M} = \begin{pmatrix} \cos\tilde{\psi}_M \cdot \cos\tilde{\varphi}_M \\ \cos\tilde{\psi}_M \cdot \sin\tilde{\varphi}_M \\ \sin\tilde{\psi}_M \end{pmatrix}$, for the small toroidal surface $\overrightarrow{n_S} = \begin{pmatrix} \cos\tilde{\psi}_S \cdot \cos\tilde{\varphi}_S \\ \sin\tilde{\psi}_S \\ \cos\tilde{\psi}_S \cdot \sin\tilde{\varphi}_S \end{pmatrix}$, for the large toroidal surface we have $\overrightarrow{n_L} = \begin{pmatrix} \sin\tilde{\psi}_L \\ \cos\tilde{\psi}_L \cdot \sin\tilde{\varphi}_L \\ \cos\tilde{\psi}_L \cdot \cos\tilde{\varphi}_L \end{pmatrix}$.

Accordingly, the scalar products $\left(\overrightarrow{N_i M_j} \cdot \overrightarrow{n_j}\right)$ will take the following nine different values for the corresponding indexes i and j:

$$\left(\overrightarrow{N_S M_S} \cdot \overrightarrow{n_S}\right) = \Big(\big(R_S + r_S \cdot \cos\tilde{\psi}_S\big) \cdot \cos\tilde{\varphi}_S - (R_S + r_S \cdot \cos\psi_S) \times \cos\varphi_S\Big) \cdot \cos\tilde{\psi}_S \cdot \cos\tilde{\varphi}_S + \big(r_S \cdot \sin\tilde{\psi}_S - r_S \cdot \sin\psi_S\big) \cdot \sin\tilde{\psi}_S + \Big(\big(R_S + r_S \cdot \cos\tilde{\psi}_S\big) \cdot \sin\tilde{\varphi}_S - (R_S + r_S \cdot \cos\psi_S) \cdot \sin\varphi_S\Big) \times \cos\tilde{\psi}_S \cdot \sin\tilde{\varphi}_S, \tag{16}$$

$$\left(\overrightarrow{N_M M_S} \cdot \overrightarrow{n_S}\right) = \Big(\big(R_S + r_S \cdot \cos\tilde{\psi}_S\big) \cdot \cos\tilde{\varphi}_S - (R_M + r_M \cdot \cos\psi_M) \times \cos\varphi_M\Big) \cdot \cos\tilde{\psi}_S \cdot \cos\tilde{\varphi}_S + \Big(r_S \cdot \sin\tilde{\psi}_S - (R_M + r_M \cdot \cos\psi_M) \times \sin\varphi_M\Big) \cdot \sin\tilde{\psi}_S + \Big(\big(R_S + r_S \cdot \cos\tilde{\psi}_S\big) \cdot \sin\tilde{\varphi}_S - r_M \cdot \sin\psi_M\Big) \times \cos\tilde{\psi}_S \cdot \sin\tilde{\varphi}_S, \tag{17}$$

$$\left(\overrightarrow{N_L M_S} \cdot \overrightarrow{n_S}\right) = \Big(\big(R_S + r_S \cdot \cos\tilde{\psi}_S\big) \cdot \cos\tilde{\varphi}_S - r_L \cdot \sin\psi_L\Big) \times \cos\tilde{\psi}_S \cdot \cos\tilde{\varphi}_S + \big(r_S \cdot \sin\tilde{\psi}_S - (R_L + r_L \cdot \cos\psi_L) \cdot \sin\varphi_L\big) \times \sin\tilde{\psi}_S + \Big(\big(R_S + r_S \cdot \cos\tilde{\psi}_S\big) \cdot \sin\tilde{\varphi}_S - (R_L + r_L \cdot \cos\psi_L) \times \cos\varphi_L\Big) \cdot \cos\tilde{\psi}_S \cdot \sin\tilde{\varphi}_S, \tag{18}$$

$$\left(\overrightarrow{N_S M_M} \cdot \overrightarrow{n_M}\right) = \Big(\big(R_M + r_M \cdot \cos\tilde{\psi}_M\big) \cdot \cos\tilde{\varphi}_M - \big(R_S + r_S \times \cos\psi_S\big) \cdot \cos\varphi_S\Big) \cdot \cos\tilde{\psi}_M \cdot \cos\tilde{\varphi}_M + \Big(\big(R_M + r_M \cdot \cos\tilde{\psi}_M\big) \times \sin\tilde{\varphi}_M - r_S \cdot \sin\psi_S\Big) \cdot \cos\tilde{\psi}_M \cdot \sin\tilde{\varphi}_M + \big(r_M \cdot \sin\tilde{\psi}_M - (R_S + r_S \cdot \cos\psi_S) \cdot \sin\varphi_S\big) \cdot \sin\tilde{\psi}_M, \tag{19}$$

$$\left(\overrightarrow{N_M M_M} \cdot \overrightarrow{n_M}\right) = \Big(\big(R_M + r_M \cdot \cos\tilde{\psi}_M\big) \cdot \cos\tilde{\varphi}_M - \big(R_M + r_M \times \cos\psi_M\big) \cdot \cos\varphi_M\Big) \cdot \cos\tilde{\psi}_M \cdot \cos\tilde{\varphi}_M + \Big(\big(R_M + r_M \cdot \cos\tilde{\psi}_M\big) \times \sin\tilde{\varphi}_M - (R_M + r_M \cdot \cos\psi_M) \cdot \sin\varphi_M\Big) \cdot \cos\tilde{\psi}_M \cdot \sin\tilde{\varphi}_M + \big(r_M \cdot \sin\tilde{\psi}_M - r_M \cdot \sin\psi_M\big) \cdot \sin\tilde{\psi}_M, \tag{20}$$

$$\left(\overrightarrow{N_L M_M} \cdot \overrightarrow{n_M}\right) = \Big(\big(R_M + r_M \cdot \cos\tilde{\psi}_M\big) \cdot \cos\tilde{\varphi}_M - r_L \cdot \sin\psi_L\Big) \times \cos\tilde{\psi}_M \cdot \cos\tilde{\varphi}_M + \Big(\big(R_M + r_M \cdot \cos\tilde{\psi}_M\big) \cdot \sin\tilde{\varphi}_M - (R_L + r_L \times \cos\psi_L) \cdot \sin\varphi_L\Big) \cdot \cos\tilde{\psi}_M \cdot \sin\tilde{\varphi}_M + \Big(r_M \cdot \sin\tilde{\psi}_M - (R_L + r_L \times \cos\psi_L) \cdot \cos\varphi_L\Big) \cdot \sin\tilde{\psi}_M, \tag{21}$$

$$\left(\overrightarrow{N_S M_L} \cdot \overrightarrow{n_L}\right) = \big(r_L \cdot \sin\tilde{\psi}_L - (R_S + r_S \cdot \cos\psi_S) \cdot \cos\varphi_S\big) \times \sin\tilde{\psi}_L + \Big(\big(R_L + r_L \cdot \cos\tilde{\psi}_L\big) \cdot \sin\tilde{\varphi}_L - r_S \cdot \sin\psi_S\Big) \cdot \cos\tilde{\psi}_L \times \sin\tilde{\varphi}_L + \Big(\big(R_L + r_L \cdot \cos\tilde{\psi}_L\big) \cdot \cos\tilde{\varphi}_L - (R_S + r_S \cdot \cos\psi_S) \times \sin\varphi_S\Big) \cdot \cos\tilde{\psi}_L \cdot \cos\tilde{\varphi}_L, \tag{22}$$

$$\left(\overrightarrow{N_M M_L} \cdot \overrightarrow{n_L}\right) = \big(r_L \cdot \sin\tilde{\psi}_L - (R_M + r_M \cdot \cos\psi_M) \cdot \cos\varphi_M\big) \times \sin\tilde{\psi}_L + \Big(\big(R_L + r_L \cdot \cos\tilde{\psi}_L\big) \cdot \sin\tilde{\varphi}_L - \big(R_M + r_M \cdot \cos\psi_M\big) \times \sin\varphi_M\Big) \cdot \cos\tilde{\psi}_L \cdot \sin\tilde{\varphi}_L + \Big(\big(R_L + r_L \cdot \cos\tilde{\psi}_L\big) \cdot \cos\tilde{\varphi}_L - r_M \cdot \sin\psi_M\Big) \cdot \cos\tilde{\psi}_L \cdot \cos\tilde{\varphi}_L, \tag{23}$$

$$\left(\overrightarrow{N_L M_L} \cdot \overrightarrow{n_L}\right) = \big(r_L \cdot \sin\tilde{\psi}_L - r_L \cdot \sin\psi_L\big) \cdot \sin\tilde{\psi}_L + \Big(\big(R_L + r_L \times \cos\tilde{\psi}_L\big) \cdot \sin\tilde{\varphi}_L - (R_L + r_L \cdot \cos\psi_L) \cdot \sin\varphi_L\Big) \cdot \cos\tilde{\psi}_L \cdot \sin\tilde{\varphi}_L + \Big(\big(R_L + r_L \cdot \cos\tilde{\psi}_L\big) \cdot \cos\tilde{\varphi}_L - (R_L + r_L \cdot \cos\psi_L) \cdot \cos\varphi_L\Big) \times \cos\tilde{\psi}_L \cdot \cos\tilde{\varphi}_L. \tag{24}$$

For specific index values i and j, we will have the following nine vector expressions $\overrightarrow{\tau_{ij}}$:

$$\overrightarrow{\tau_{SS}} = \begin{pmatrix} \left(R_S + r_S \cdot \cos\tilde{\psi}_S\right) \cdot \cos\tilde{\varphi}_S - \left(R_S + r_S \cdot \cos\psi_S\right) \cdot \cos\varphi_S - \left(\overrightarrow{N_S M_S} \cdot \overrightarrow{n_S}\right) \cdot \cos\tilde{\psi}_S \cdot \cos\tilde{\varphi}_S \\ r_S \cdot \sin\tilde{\psi}_S - r_S \cdot \sin\psi_S - \left(\overrightarrow{N_S M_S} \cdot \overrightarrow{n_S}\right) \cdot \sin\tilde{\psi}_S \\ \left(R_S + r_S \cdot \cos\tilde{\psi}_S\right) \cdot \sin\tilde{\varphi}_S - \left(R_S + r_S \cdot \cos\psi_S\right) \cdot \sin\varphi_S - \left(\overrightarrow{N_S M_S} \cdot \overrightarrow{n_S}\right) \cdot \cos\tilde{\psi}_S \cdot \sin\tilde{\varphi}_S \end{pmatrix}, \tag{25}$$

$$\overrightarrow{\tau_{MS}} = \begin{pmatrix} \left(R_S + r_S \cdot \cos\tilde{\psi}_S\right) \cdot \cos\tilde{\varphi}_S - \left(R_M + r_M \cdot \cos\psi_M\right) \cdot \cos\varphi_M - \left(\overrightarrow{N_M M_S} \cdot \overrightarrow{n_S}\right) \cdot \cos\tilde{\psi}_S \cdot \cos\tilde{\varphi}_S \\ r_S \cdot \sin\tilde{\psi}_S - \left(R_M + r_M \cdot \cos\psi_M\right) \cdot \sin\varphi_M - \left(\overrightarrow{N_M M_S} \cdot \overrightarrow{n_S}\right) \cdot \sin\tilde{\psi}_S \\ \left(R_S + r_S \cdot \cos\tilde{\psi}_S\right) \cdot \sin\tilde{\varphi}_S - r_M \cdot \sin\psi_M - \left(\overrightarrow{N_M M_S} \cdot \overrightarrow{n_S}\right) \cdot \cos\tilde{\psi}_S \cdot \sin\tilde{\varphi}_S \end{pmatrix}, \tag{26}$$

$$\overrightarrow{\tau_{LS}} = \begin{pmatrix} \left(R_S + r_S \cdot \cos\tilde{\psi}_S\right) \cdot \cos\tilde{\varphi}_S - r_L \cdot \sin\psi_L - \left(\overrightarrow{N_L M_S} \cdot \overrightarrow{n_S}\right) \cdot \cos\tilde{\psi}_S \cdot \cos\tilde{\varphi}_S \\ r_S \cdot \sin\tilde{\psi}_S - \left(R_L + r_L \cdot \cos\psi_L\right) \cdot \sin\varphi_L - \left(\overrightarrow{N_L M_S} \cdot \overrightarrow{n_S}\right) \cdot \sin\tilde{\psi}_S \\ \left(R_S + r_S \cdot \cos\tilde{\psi}_S\right) \cdot \sin\tilde{\varphi}_S - \left(R_L + r_L \cdot \cos\psi_L\right) \cdot \cos\varphi_L - \left(\overrightarrow{N_L M_S} \cdot \overrightarrow{n_S}\right) \cdot \cos\tilde{\psi}_S \cdot \sin\tilde{\varphi}_S \end{pmatrix}, \tag{27}$$

$$\overrightarrow{\tau_{SM}} = \begin{pmatrix} \left(R_M + r_M \cdot \cos\tilde{\psi}_M\right) \cdot \cos\tilde{\varphi}_M - \left(R_S + r_S \cdot \cos\psi_S\right) \cdot \cos\varphi_S - \left(\overrightarrow{N_S M_M} \cdot \overrightarrow{n_M}\right) \cdot \cos\tilde{\psi}_M \cdot \cos\tilde{\varphi}_M \\ \left(R_M + r_M \cdot \cos\tilde{\psi}_M\right) \cdot \sin\tilde{\varphi}_M - r_S \cdot \sin\psi_S - \left(\overrightarrow{N_S M_M} \cdot \overrightarrow{n_M}\right) \cdot \cos\tilde{\psi}_M \cdot \sin\tilde{\varphi}_M \\ r_M \cdot \sin\tilde{\psi}_M - \left(R_S + r_S \cdot \cos\psi_S\right) \cdot \sin\varphi_S - \left(\overrightarrow{N_S M_M} \cdot \overrightarrow{n_M}\right) \cdot \sin\tilde{\psi}_M \end{pmatrix}, \tag{28}$$

$$\overrightarrow{\tau_{MM}} = \begin{pmatrix} \left(R_M + r_M \cdot \cos\tilde{\psi}_M\right) \cdot \cos\tilde{\varphi}_M - \left(R_M + r_M \cdot \cos\psi_M\right) \cdot \cos\varphi_M - \left(\overrightarrow{N_M M_M} \cdot \overrightarrow{n_M}\right) \cdot \cos\tilde{\psi}_M \cdot \cos\tilde{\varphi}_M \\ \left(R_M + r_M \cdot \cos\tilde{\psi}_M\right) \cdot \sin\tilde{\varphi}_M - \left(R_M + r_M \cdot \cos\psi_M\right) \cdot \sin\varphi_M - \left(\overrightarrow{N_M M_M} \cdot \overrightarrow{n_M}\right) \cdot \cos\tilde{\psi}_M \cdot \sin\tilde{\varphi}_M \\ r_M \cdot \sin\tilde{\psi}_M - r_M \cdot \sin\psi_M - \left(\overrightarrow{N_M M_M} \cdot \overrightarrow{n_M}\right) \cdot \sin\tilde{\psi}_M \end{pmatrix}, \tag{29}$$

$$\overrightarrow{\tau_{LM}} = \begin{pmatrix} \left(R_M + r_M \cdot \cos\tilde{\psi}_M\right) \cdot \cos\tilde{\varphi}_M - r_L \cdot \sin\psi_L - \left(\overrightarrow{N_L M_M} \cdot \overrightarrow{n_M}\right) \cdot \cos\tilde{\psi}_M \cdot \cos\tilde{\varphi}_M \\ \left(R_M + r_M \cdot \cos\tilde{\psi}_M\right) \cdot \sin\tilde{\varphi}_M - \left(R_L + r_L \cdot \cos\psi_L\right) \cdot \sin\varphi_L - \left(\overrightarrow{N_L M_M} \cdot \overrightarrow{n_M}\right) \cdot \cos\tilde{\psi}_M \cdot \sin\tilde{\varphi}_M \\ r_M \cdot \sin\tilde{\psi}_M - \left(R_L + r_L \cdot \cos\psi_L\right) \cdot \cos\varphi_L - \left(\overrightarrow{N_L M_M} \cdot \overrightarrow{n_M}\right) \cdot \sin\tilde{\psi}_M \end{pmatrix}, \tag{30}$$

$$\overrightarrow{\tau_{SL}} = \begin{pmatrix} r_L \cdot \sin\tilde{\psi}_L - \left(R_S + r_S \cdot \cos\psi_S\right) \cdot \cos\varphi_S - \left(\overrightarrow{N_S M_L} \cdot \overrightarrow{n_L}\right) \cdot \sin\tilde{\psi}_L \\ \left(R_L + r_L \cdot \cos\tilde{\psi}_L\right) \cdot \sin\tilde{\varphi}_L - r_S \cdot \sin\psi_S - \left(\overrightarrow{N_S M_L} \cdot \overrightarrow{n_L}\right) \cdot \cos\tilde{\psi}_L \cdot \sin\tilde{\varphi}_L \\ \left(R_L + r_L \cdot \cos\tilde{\psi}_L\right) \cdot \cos\tilde{\varphi}_L - \left(R_S + r_S \cdot \cos\psi_S\right) \cdot \sin\varphi_S - \left(\overrightarrow{N_S M_L} \cdot \overrightarrow{n_L}\right) \cdot \cos\tilde{\psi}_L \cdot \cos\tilde{\varphi}_L \end{pmatrix}, \tag{31}$$

$$\overrightarrow{\tau_{ML}} = \begin{pmatrix} r_L \cdot \sin\tilde{\psi}_L - \left(R_M + r_M \cdot \cos\psi_M\right) \cdot \cos\varphi_M - \left(\overrightarrow{N_M M_L} \cdot \overrightarrow{n_L}\right) \cdot \sin\tilde{\psi}_L \\ \left(R_L + r_L \cdot \cos\tilde{\psi}_L\right) \cdot \sin\tilde{\varphi}_L - \left(R_M + r_M \cdot \cos\psi_M\right) \cdot \sin\varphi_M - \left(\overrightarrow{N_M M_L} \cdot \overrightarrow{n_L}\right) \cdot \cos\tilde{\psi}_L \cdot \sin\tilde{\varphi}_L \\ \left(R_L + r_L \cdot \cos\tilde{\psi}_L\right) \cdot \cos\tilde{\varphi}_L - r_M \cdot \sin\psi_M - \left(\overrightarrow{N_M M_L} \cdot \overrightarrow{n_L}\right) \cdot \cos\tilde{\psi}_L \cdot \cos\tilde{\varphi}_L \end{pmatrix}, \tag{32}$$

$$\overrightarrow{\tau_{LL}} = \begin{pmatrix} r_L \cdot \sin\tilde{\psi}_L - r_L \cdot \sin\psi_L - \left(\overrightarrow{N_L M_L} \cdot \overrightarrow{n_L}\right) \cdot \sin\tilde{\psi}_L \\ \left(R_L + r_L \cdot \cos\tilde{\psi}_L\right) \cdot \sin\tilde{\varphi}_L - \left(R_L + r_L \cdot \cos\psi_L\right) \cdot \sin\varphi_L - \left(\overrightarrow{N_L M_L} \cdot \overrightarrow{n_L}\right) \cdot \cos\tilde{\psi}_L \cdot \sin\tilde{\varphi}_L \\ \left(R_L + r_L \cdot \cos\tilde{\psi}_L\right) \cdot \cos\tilde{\varphi}_L - \left(R_L + r_L \cdot \cos\psi_L\right) \cdot \cos\varphi_L - \left(\overrightarrow{N_L M_L} \cdot \overrightarrow{n_L}\right) \cdot \cos\tilde{\psi}_L \cdot \cos\tilde{\varphi}_L \end{pmatrix}. \tag{33}$$

Since the equality $\overrightarrow{E_{\tau j}} = \overrightarrow{0}$ must be fulfilled at all points M_j of all three toroidal surfaces, the search for densities of q_i charge distributions can be reduced to minimizing the functional equal to the sum of three integrals over the tori surfaces from the length square of the vector that should turn to be zero:

$$\sum_{j=S,M,L} r_j \int_0^{\pi} \left(R_j + r_j \cos\tilde{\psi}_j\right) d\tilde{\psi}_j \int_0^{\pi/2} \Big(\sum_{i=S,M,L} r_i \int_0^{2\pi} (R_i + r_i \cos\psi_i) d\psi_i \int_0^{2\pi} \frac{q_i \cdot \overrightarrow{\tau_{ij}}}{|N_i M_j|^3} d\varphi_i \Big)^2 d\tilde{\varphi}_j. \tag{34}$$

In the last two cases, the integrations are not carried over full turns due to the octahedral symmetry of the problem.

To solve the problem of minimizing the functional numerically, all four definite integrals were replaced by sums according to the quadrature formula of the average rectangles. Taking into account the limited computer resources, during numerical integration, the nodes were located from each other with an interval of 3°. To avoid division by zero, the nodes for variables $\varphi_i = \pi\alpha_i/60$ and $\tilde{\varphi}_j = \pi\,(3\tilde{\alpha}_j + 1.5)/180$ and, respectively, $\psi_i = \pi\beta_i/60$ and $\tilde{\psi}_j = \pi\left(3\tilde{\beta}_j + 1.5\right)/180$, were taken with a shift of one and a half degrees. As a result, the expression was minimized

$$f\,(q_i) = \sum_{j=S,M,L} r_j \sum_{\tilde{\beta}_j=1}^{60} \left(R_j + r_j \cdot \cos\frac{\pi\left(3\tilde{\beta}_j + 1.5\right)}{180} \right) \times \frac{\pi}{60} \sum_{\tilde{\alpha}_j=1}^{30} \Big(\sum_{i=S,M,L} r_i \sum_{\beta_i=1}^{120} \left(R_i + r_i \cdot \cos\frac{\pi\beta_i}{60} \right) \times \frac{\pi}{60} \sum_{\alpha_i=1}^{120} \frac{q_i \cdot \overrightarrow{\tau_{ij}}}{|N_i M_j|^3} \cdot \frac{\pi}{60} \Big)^2 \cdot \frac{\pi}{60}. \tag{35}$$

The resulting function of $3 \times 120 \times 120 = 43\,200$ variables was minimized by method of gradient descent. This method is an iterative numerical method for solving optimization problems. It is characterized by simplicity of calculations and weak requirements for the minimized function [17], although it is not optimal [18]. If there were no octahedral symmetry, then in this problem, in order to apply the gradient descent method, it would be necessary to have expressions of all 43 200 partial derivatives of this minimized function. Actually only $43\,200 : 8 = 5400$ of such derivative are calculated:

$$\frac{\partial f}{\partial q_m} = \sum_{j=S,M,L} r_j \sum_{\tilde{\beta}_j=1}^{60} \left(R_j + r_j \cdot \cos\frac{\pi\left(3\tilde{\beta}_j + 1.5\right)}{180} \right) \times \frac{\pi}{60} \sum_{\tilde{\alpha}_j=1}^{30} \left(\sum_{i=S,M,L} r_i \sum_{\beta_i=1}^{120} \left(R_i + r_i \cdot \cos\frac{\pi\beta_i}{60} \right) \times \frac{\pi}{60} \sum_{\alpha_i=1}^{120} \frac{q_i \cdot \overrightarrow{\tau_{ij}}}{|N_i M_j|^3} \frac{\pi}{60} r_m \left(R_m + r_m \cdot \cos\frac{\pi\beta_m}{60} \right) \times \frac{\pi}{60} \frac{\overrightarrow{\tau_{mj}}}{|N_m M_j|^3} \cdot \frac{\pi}{60} \right) \cdot \frac{\pi}{60}. \tag{36}$$

Uniform charge distributions over each of the toroidal surfaces were used as an initial approximation. I.e. if on the i-th toroidal surface the charge Q_i was initially distributed, then, it was assumed that $q_i(\varphi_i, \psi_i) = Q_i/S_i$, where $S_i = 4\pi^2 R_i r_i$ is the area of i-th toroidal surface.

The new value of the charge distribution density was found by the formula

$$q_i^{new} = q_i^{old} - L \cdot \frac{\partial f}{\partial q_i}, \tag{37}$$

where L is a small positive hyperparameter selected empirically in test calculations. During each iteration of the gradient descent method, the calculated total amount of charge on each of the toroidal surfaces was changed, which can be found using the approximate formula

$$Q_i^{new} = r_i \sum_{\beta_i=1}^{120} \left(R_i + r_i \cos\frac{\pi\beta_i}{60} \right) \cdot \frac{\pi}{60} \sum_{\alpha_i=1}^{120} q_i^{new} \frac{\pi}{60}. \tag{38}$$

Since, in fact, the amount of charge remained unchanged, before the next iteration, the value q_i^{new} had to be adjusted by distributing the missing part of the charge evenly over the entire surface

$$q_i = q_i^{new} + \frac{Q_i^{old} - Q_i^{new}}{S_i}. \tag{39}$$

2. Computer simulation results

The results of numerical calculations are given for structures with relative dimensions $R_S : R_M : R_L : r_S : r_M : r_L = 3 : 6 : 9 : 1 : 1 : 1$. The graphs show the charge distribution densities for the case when the unit charge was applied only to the medium torus, and there were no charges on the small and large tori. These densities are measured in units equal to the ratio of the charge applied to the medium torus to the square of the radius of the tori forming the circles (all three radii were the same in calculations).

Figure 3 shows the charge distribution density q_M at the points of the medium toroidal surface depending on the angle ψ_M. The left part of the graphs ($\psi_M = 0$) corresponds to the points located further from the center of the torus, and the right part ($\psi_M = \pi$) corresponds to the points that are located closer to the center. The uncharged large and small tori attract the charges of the medium torus. Graph *1* corresponds to the cross-section $\varphi_M = \pi/2$ which is maximally close to the large torus, while graph *2* — to the cross-section $\varphi_M = 0$ maximally close to the small torus . These results are quite expected, since the „dipole“ is induced on an uncharged conductor, which reciprocally attracts the charges that generated it. If there were neither small nor large tori, but only one charged medium one, then the tension graph would look like a curve practically connecting the lower parts of the graphs shown. This is completely consistent with the fact that the charges, repelling each other, are distributed with greater concentration on the outer parts of the charged body.

Figure 4 shows the charge distribution density q_M at the points of the medium toroidal surface depending on the angle φ_M.

It is known from electrostatics that charges tend to concentrate in areas with maximum positive curvature, especially those located further from the center. The results obtained fully correspond to it. Graph *4* corresponds to „external“ circumference of toroidal surface which is most remote from the center, and graph *3* — to „internal“ circumference. If there were no small and large tori, then both of these lines would turn out to be horizontal lines running at the minimum levels of the graphs shown. The right part of the graph *4* turns out to be higher because it approaches the large torus, which, although not charged, is itself a dipole due to the redistribution of charges and attracts the charges. For a similar reason, due to the approach to the small torus, the graph *3* has an elevation in the left part.

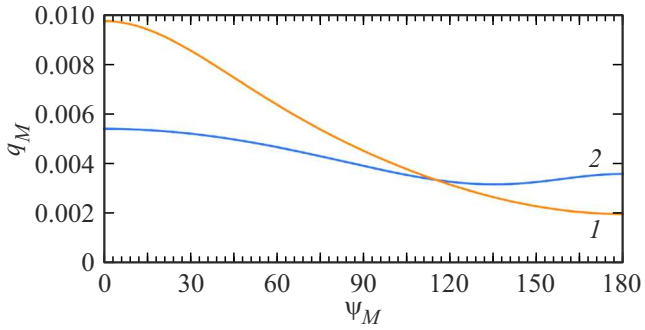

Figure 3. Charge distribution density on the surface of the medium torus versus „radial“ coordinate.

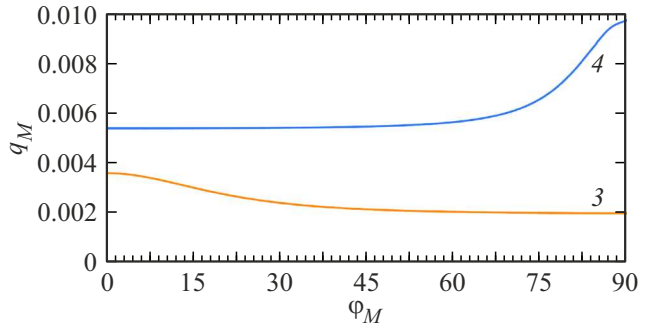

Figure 4. Charge distribution density on the surface of a medium torus versus „circumferential“ coordinate.

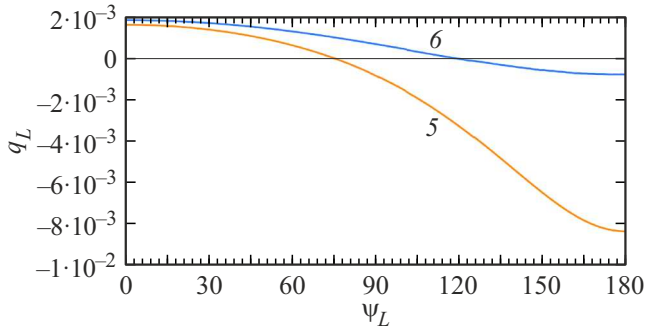

Figure 5. Induced charge distribution density on the surface of an uncharged large torus versus „radial“ coordinate.

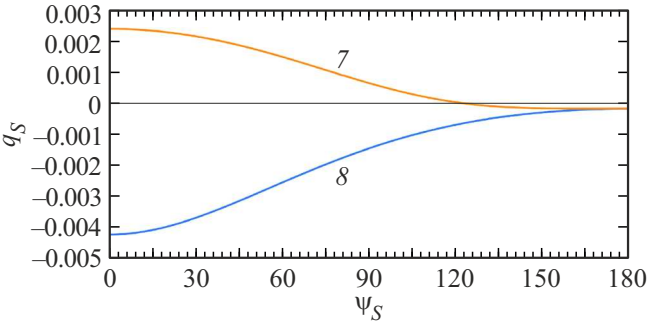

Figure 6. Induced charge distribution density on the surface of an uncharged large torus versus „radial“ coordinate.

Figures 5–8 show the dependences of the charge distribution density on uncharged (i.e., having total zero charges) large and small tori. The results obtained fully correspond to the physical concept. For example, in Fig. 5 and 6 the graphs *5* and *8*, located below the graphs *6* and *7* correspond to the cross sections that are as close as possible to the charged medium torus. Moreover, in both cases, the maximum modulus charge of the opposite sign is induced on the side (inner, where $\psi_L = \pi$, for the large torus, and outer, where $\psi_S = 0$, — for the small torus), which turns out to be closer to the charged medium torus.

In Figures 7 and 8, the graphs *10* and *11*, which differ little from the horizontal lines, correspond to the tori circumferences maximally distant from the charged medium torus, i.e., for the large torus — to the outer circumference, and for the small torus — to the inner circumference. The graphs *9* and *12* correspond to the circumferences of the tori closest to the charged medium torus. And, of course,

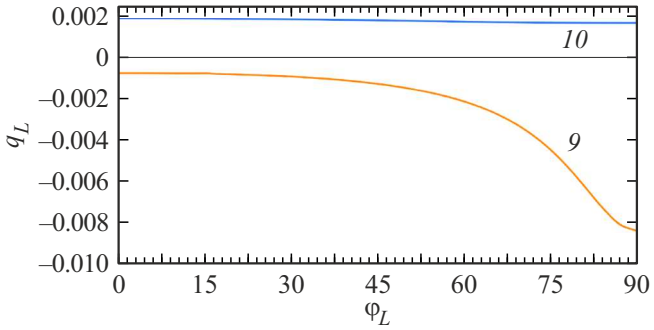

Figure 7. Induced charge distribution density on the surface of an uncharged large torus versus „circumferential" coordinate.

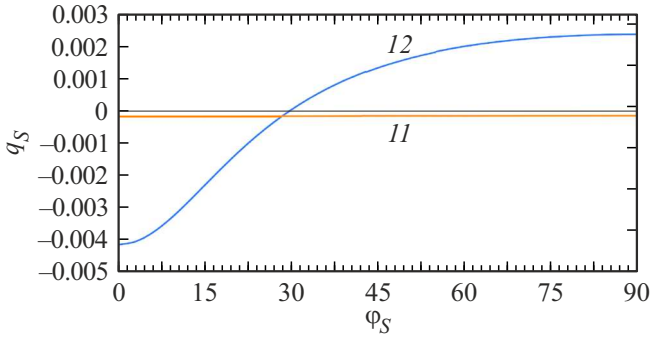

Figure 8. Induced charge distribution density on the surface of an uncharged small torus versus „circumferential" coordinate.

the parts of these graphs where the charge takes on negative values correspond to those parts of the circumferences that are closer to the charged medium torus. For the large torus these points lie in the vicinity of value $\varphi_L = \pi/2$, and for the small torus — the points are located in the vicinity of value $\varphi_S = 0$.

Fig. 9 for all of the three tori illustrates the side view. For the large torus it corresponds to the view form the end of Ox axis, for the medium torus — to the view from the end of Oz axis, for the small torus — to the view from the end of Oy axis.

The horizontal segments between the small and medium tori correspond to the sections of the Ox axis, and the vertical segments between the medium and large tori correspond to Oy axis. The isolines on the tori, drawn with a step of 0.001, correspond to the same values of the charge distribution density. The isolines corresponding to zero charge density are marked with pointers. Fig.9 demonstrates that on the medium torus, maximum density of isolines occurs on its outer parts near Oy axis, i.e., near the large torus, whereas minimum density occurs on the inner part of the torus. The mutual influence of charges located on the medium torus and induced on the large torus is manifested in the fact that the density of isolines on the large torus reaches the highest values near the medium torus.

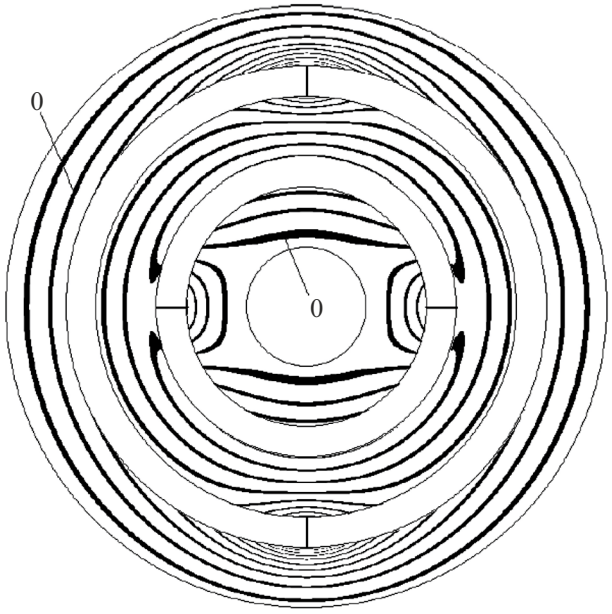

Figure 9. Isolines of the charge distribution density on the surfaces of the tori.

Conclusion

The findings of the study allow us making a conclusion on the possibility of solving the problems of electrostatic charges distribution densities on one or a small number of conducting bodies with smooth surfaces using an iterative numerical method that minimizes the tangential components of stresses on the surfaces of these bodies. The classical gradient descent method was used in this study, which does not claim competitive advantages in terms of speed or resource intensity, but allowed us to obtain a solution to a new relevant and quite sophisticated problem for the first time. In the future, the authors plan to improve the calculation methodology in order to reduce computational costs. In particular, artificial intelligence is planned to be used.

Funding

This study was supported by the Russian Science Foundation, grant № 24-21-00104, https://rscf.ru/project/24-21-00104/

Conflict of interest

The authors declare that they have no conflict of interest.

References

[1] E.I. Vorobyov, E.E. Kovalev. *Radiatsionnaya bezopasnost ekipazhei letatel'nykh apparatov* (Energoatomizdat, M., 1983), 152 p. (in Russian).

[2] E.E. Kovalev, E.D. Molchanov, Yu.G. Pekhterev, T.Ya. Ryabova, B.I. Tikhomirov, A.I. Khovanskaya. Kosmicheskiye issledovania, **13** (5), 771 (1975) (in Russian).
[3] E.E. Kovalev, E.D. Molchanov, Yu.G. Pekhterev, T.Ya. Ryabova, B.I. Tikhomirov, A.I. Khovanskaya. Kosmicheskiye issledovania, **14** (1), 126 (1976) (in Russian).
[4] A.G. Rebeko. Inzhenerny zhurnal: nauka i innovatsii, **5**, 1 (2016). (in Russian).
[5] T.Ya. Ryabova. Kosmicheskaya biologiya i aviakosmicheskaya meditsina, **17** (2), 4 (1983) (in Russian).
[6] V.V. Tsetlin, V.I. Pavlushkina, V.I. Redko. Kosmicheskiye issledovania, **33** (3), 286 (1995) (in Russian).
[7] E.E. Kovalev, V.M. Petrov, V.V. Markelov, T.Ya. Ryabova, V.V. Benchin, I.V. Chernykh. *Osnovniye itogi i perspekivi issledovaniy na stantsiyakh „Prognoz" po operativnomu obespecheniyu radiatsionnoy bezopasnosti kosmicheskikh poletov*. Summary report 5 nauchn. chteniya po kosmonavtike (Nauka, M., 1984), p. 196–206 (in Russian).
[8] Yu.A. Akatov, V.E. Dudkin, E.E. Kovalev. et.al. Nucl. Tracks Radiat. Meas., **17** (2), 105 (1990).
[9] E.E. Kovalev, E.D. Molchanov, V.K. Lebedev, T.Ya. Ryabova, Yu.G. Pekhterev, A.V. Kolodin, G.I. Leskov. Kosmicheskiye issledovania, **25** (4), 585 (1987) (in Russian).
[10] J.C. Sussingham, S.A. Watkins, F.H. Cocks. J. Astronautical Sc., **47** (3,4), 165 (1999). DOI: 10.1007/BF03546197
[11] P.T. Metzger, J.E. Lane, R.C. Youngquist. *Progress Toward Electrostatic Radiation Shielding of Interplanetary Spacecraft / Strategies, Concepts and Technical Challenges of Human Exploration Beyond Low Earth Orbit Paper Session II-B* (41st) (Space Congress Proceedings, 6, 2004).
[12] J.G. Smith, T. Smith, M. Williams, R. Youngquist, W. Mendell. *Potential Polymeric Sphere Construction Materials for a Spacecraft Electrostatic Shield. NASA/TM* (2006, 214302), https://ntrs.nasa.gov/search.jsp?R=20060013423
[13] R.P. Joshi, H. Qiu, R.K. Tripathi. Acta Astronautica, **88**, 138 (2013).
[14] P.T. Metzger, J.E. Lane. Open Appl. Phys. J., **2**, 32 (2009).
[15] Yu.N. Tashaev. Uspekhi prikladnoi fiziki, **3** (2), 126 (2015) (in Russian).
[16] L.D. Landau, E.M. Lifshitz. *Teoreticheskaya phisika*: uch.posob.dlya vuzov *Elektrodinamika sploshnykh sred.* (Fizmatlit, M., 2005), in 10 v., v. VIII, 4-th ed. stereotyp. (in Russian).
[17] B.T. Polyak. *Vvedenie v optimizatsiyu* (Nauka, M., 1983), 384 p (in Russian).
[18] Yu.E. Nesterov. *Vvedenie v vypukluyu optimizatsiyu* (MTsIMO, M., 2010), 280 p. (in Russian).

Translated by T.Zorina